

Comparative analysis of recent metaheuristic algorithms for maximum power point tracking of solar photovoltaic systems under partial shading conditions

Suraj Ravi¹, Manoharan Premkumar¹, Laith Abualigah^{2,3,4,5}

¹Department of Electrical and Electronics Engineering, Dayananda Sagar College of Engineering, Bengaluru, India

²Computer Science Department, Prince Hussein Bin Abdullah Faculty for Information Technology, Al-Bayt University, Mafrq, Jordan

³Hourani Center for Applied Scientific Research, Al-Ahliyya Amman University, Amman, Jordan

⁴MEU Research Unit, Middle East University, Amman, Jordan

⁵School of Computer Sciences, Universiti Sains Malaysia, Pulau Pinang, Malaysia

Article Info

Article history:

Received Jan 23, 2023

Revised Apr 11, 2023

Accepted Apr 17, 2023

Keywords:

Boost converter

Metaheuristic algorithm

MPPT algorithms

Partial shading conditions

ABSTRACT

The photovoltaic (PV) system comprises one or more solar panels, a converter/inverter, controllers, and other mechanical and electrical elements that utilize the generated electrical energy by the PV modules. The PV systems are ranged from small roofs or transportable units to massive electric utility plants. The maximum power point tracking (MPPT) controller has been used in PV systems to get the maximum power available. In addition, the MPPT controller is much essential for PV systems to protect the battery devices or direct loads from the power fluctuations received from solar PV panels. There are several MPPT control mechanisms available right now. The most common and commonly applied approaches under constant irradiance are perturb and observe (P&O) and incremental conductance (INC). But such methods show variations in the maximum power point. In this sense, this paper analyses and utilizes two recent metaheuristic algorithms called artificial rabbit optimization (ARO) and the most valuable player (MVP) algorithm for MPPT applications. The performance comparisons are made with the most preferred traditional algorithms, such as P&O and INC. Based on the result obtained, this study recommends that ARO perform better in standard testing conditions than all the other algorithms, but in partially shaded conditions, the MVP algorithm performs better in terms of efficiency and tracking speed.

This is an open access article under the [CC BY-SA](https://creativecommons.org/licenses/by-sa/4.0/) license.



Corresponding Author:

Manoharan Premkumar

Department of Electrical and Electronics Engineering, Dayananda Sagar College of Engineering

Bengaluru, Karnataka 560078, India

Email: mprem.me@gmail.com.

1. INTRODUCTION

Solar power generation is rapidly expanding in many regions worldwide, owing to cost reductions, economic incentives, and the need to fulfil rising energy demand while reducing reliance on fossil fuels. However, various problems must be overcome before they can be considered significant. The power production of solar photovoltaic (PV) arrays, solar irradiation, and PV array efficiency can suffer significantly when partially shaded. Shading can be produced by various factors, including clouds, buildings, trees, soiling, dust, and even PV cell splitting and ageing. The extent and influence of shading vary according to the application and end use, for example, solar PV power plants, building-integrated photovoltaics, rural electrification, or electric cars. Reducing the effect of partial shadowing is a significant practical difficulty.

Partial shadowing reduces the power output of the PV array while also causing the power-voltage (P-V) curve to have several peaks. As a result, standard maximum power point tracking (MPPT) may become caught at the local maximum power point (LMPP), resulting in severe power losses. Various traditional MPPT algorithms under partial shade have been developed to solve this issue and their categorization. To approach the global maximum power point (GMPP), notable recent contributions include fuzzy-logic controllers, neural-network-based techniques, and advanced evolutionary algorithms. The complexity and expense of these algorithms and the requirement for integrated sensors in some circumstances remain some of the fundamental difficulties. The need for renewable and pollution-free energy sources leads to the development of transformation systems utilizing renewables, and fuel cells. Photovoltaic (PV) power generation is developing rapidly as the cost of PV power generation reduces greatly over a period of time [1]. The key point of this study is that the PV model is obtained using design data from the manufacturer's datasheet. As a result, the model gives more accurate results than the built-in PV array model in the MATLAB programme [2]. Because the I-V relation for the PV array is determined, the model with five parameters was built. The resulting PV model is adaptable for all PV parameters and P-V and I-V for the PV array. The accuracy and reliability of the PV model are validated routinely by comparing simulation results to data supplied by the manufacturers. The generated model requires data from the manufacturer's datasheet. The suggested model's qualities, such as dependability, precision, and flexibility, allow the designers to forecast, and it also describes the best possible algorithm suitable for partially shaded conditions [3], [4].

Artificial bee colony (ABC) was used to precisely measure and estimate the characteristics of solar cells, and it has been presented. The estimating procedure is described as an optimization concern in the methodology. As a primary solution, the proposed approach improves the characteristics of the solar cell. The objective function evaluates the match between a prospective solution and observational results. The algorithm's efficiency has been determined by reliability [5]. Several studies have been conducted to improve its effectiveness under varying weather conditions. The development of various algorithms for tracking and extracting the most accessible power makes utilizing energy from the sun more suitable. The impact of irradiance on MPPT leads to multiple power peaks as a function of the use of photodiodes that traverse to mitigate the consequences of different shading circumstances [6]. One of the essential challenges when addressing commercial uses of PV systems is estimating the efficiency of a PV system since I-V and P-V characteristics are very nonlinear. It should be mentioned that most manufacturers' datasheets lack comprehensive information on the equivalent electrical characteristics of PV systems required to model an effective PV module [7], [8]. Due to this, the chance to select low-power peaks as maximum power by the MPPT algorithm increases. Due to local peaks, perturb and observe (P&O) and hill-climbing algorithms are examples of traditional methodologies [9]–[11].

Monitoring the maximum peak is wasteful because fluctuations around the maximum cause power outages. A modified version of the P&O methodology [7]–[9] is employed, in which the local peaks are first determined, and during the second loop, the global peak is determined, but it needs more time to compute the maximum power and hence is slower in response. MPPT algorithms that use an artificial neural network (ANN) and fuzzy control [10]–[13] are more convenient under light load conditions and in continuously monitoring peak energy, but they require more memory because vast amounts of data are required for training the network and are more complex. Various optimization techniques, such as flow-on effects and particle swarm optimization (PSO), ant colony optimization, Jaya algorithm, genetic algorithm, and so on, are used to track optimal power for the PV energy conversion system [14]–[16], which processes the entire range of voltage or duty ratio and thus determines the global peak of PV power and requires fewer data samples. As the metaheuristic algorithms track the global peak efficiently, the tracking speed, and fluctuations, are concentrated for improvement.

The PSO, flower pollination, ant colony, and firefly-based MPPT algorithms provide better tracking efficiency under various partial shading conditions, but it causes continuous perturbation, resulting in an increased number of iterations, which leads to a longer settling time and more fluctuation, resulting in higher power losses. Under uniformly distributed irradiances, a photovoltaic array's PV characteristics have a sharp peak. When the irradiance is not uniformly distributed across the PV system, the P-V contour has many spikes, referred to as partial shading conditions (PSCs). Because of their robustness in monitoring the global peak (GP) of many application areas, clustering techniques are again used as maximum power point trackers for PV under PSCs [17]–[22]. Based on PSO and differential evolutionary (DE) and Jaya algorithms, the author suggested improved MPPT algorithms for the PV system subjected to different operating conditions [23], [24]. To resolve the drawbacks of DE, the main characteristics of PSO are merged with DE. The presented hybrid maximum power point uses a random mutation loop to avoid all municipal peaks. Whenever this loop is powered up, it is determined by the maximum number of iterations. The hybrid MPPT's performance is validated using both simulation and a hardware setup. Three different PSCs were used to test the proposed methodology. The suggested technique is a step forward in this field, making the system more robust and increasing overall computational speed. It can find the true global MPP with the

exception of conventional PSO techniques. This algorithm successfully handles changes that occur in irradiance conditions and is applicable in real-time. Other algorithms, such as adaptive radial movement optimization, grey wolf-assisted P&O, chaotic flower pollination, and hybrid PSO-P&O, are proposed for the PV systems to track the maximum power point at different operating conditions [25]–[28]. Another study presents a control scheme for grid-connected photovoltaic systems based on two different three-phase topologies of multilevel inverters. Based on the bifurcation method, the investigated topologies are divided into two basic groups: Topologies of DC-DC converter and cascade inverter grid-connected PV systems are designed to be sustainable by using particle swarm optimization, and a good solution is to use two multilevel converter topologies for maximizing PV generator energy yield and improving the system's ability to meet this same requirement for power generation delivered to the grid [29]. A comprehensive study was performed in this manuscript to analyze the obstacles in the 12 GMPPT methodologies for heuristic enhancement, notably manipulative and improvisational browsing capabilities. This paper discusses that variable vortex search (VVS)-based GMPP tracking has more than 99% tracking accuracy in simulation and hardware tests. Furthermore, it diminishes computational complexity and is simple to implement. The most important existing heuristic optimization techniques are analyzed and discussed. The literary works processes and the new VVS-based GMPP strategy would then allow the researchers to pick the best strategy for their specific needs [30]–[33]. The researchers in the works [34], [35] allow us to understand the new algorithm used for partially shaded conditions based on humpback whale assisted and whale optimization for different partially shaded conditions.

A hybrid shuffled frog leaping algorithm with PSO, hybrid dragonfly and INC algorithm, hybrid P&O with ABC, and hybrid Jaya algorithm are proposed and are used to cover a large range in a shorter time period, resulting in reduced tracking time and power losses when compared to the conventional algorithms. The settling time is high, so the efficiency is low [36]–[39]. Hassan *et al.* [40] introduce novel models for predicting the power output of PV systems at various scales and in desert locations, incorporating a nonlinear autoregressive neural network to exogenous inputs with evolutionary algorithms for gradient-free training. Five models have been developed for each site, beginning with a free model and ending with the most expensive model. Hassan *et al.* [41] have proposed a new regression and ensemble-learning model for forecasting the performance of PV energy plants operating in desert regions, taking into account the innovative tools of the photovoltaic system and the character traits of the procedure settings and climatic conditions. Nwokolo *et al.* [42] developed and validated 294 physical models from six different PV power technologies using machine learning, Gumbel's probabilistic approach and hybridization of the two to aid in the possible determination of PV electric energy generation in the unique geographical and climatic environment of the experiment site.

The most valuable player (MVP) methodology [43], [44] is identified as a new algorithm and highly efficient in removing the drawbacks of traditional algorithms as well as other metaheuristic computational methods. There have been two of them working on components: the first phase is determining the best individual solution, and the next determines the most efficient approach among a group of the best possible remedies. As a result, the global peak is explored more quickly. In order to get this, a search space-limiting strategy is considered as a means of bringing down the interval of solutions. The MVP algorithm is also tested and validated using MPPT optimization problems [44]. The tracking speed, power fluctuations, and settling time are all minimized with this strategy. A new optimization technique known as artificial rabbit optimization is investigated in this work, in which the search space limitation technique from MPPT is combined with three strategies: detour foraging, random concealment, and resource dwindling [45]. The excursion foraging scheme explores all power peaks during partial shading conditions, the random hiding strategy determines the global peak, and the energy reduction framework improves its equilibrium among both the availability of the best possible duty ratio and, thus, tracking the maximum power. The following are the contributions of the paper: i) Development of MVP and artificial rabbit optimization (ARO) algorithms for MPPT applications; ii) Problem formulation to optimize the output power of the PV array; iii) Testing the algorithms using different case studies; and iv) Compare the performance of ARO and MVO with P&O and INC algorithms.

The paper is organized as follows. Section 2 discusses the mathematical modelling of the PV cell/module. In addition, the effects of the bypass diode on the PV array during partial shading conditions are also discussed. Section 3 deals with the operation of the traditional boost DC-DC converter. Section 4 discusses the formulation and mathematical modelling of MVP and ARO algorithms. Section 5 presents the simulation results under three different operating conditions. Section 6 concludes the paper.

2. MODELLING OF PHOTOVOLTAIC CELL

The equivalent 5-parameter PV cell model circuit is shown in Figure 1. It is always necessary to extract the parameters of the PV cell for proper modelling of the PV systems [46]. The PV model has five parameters: Photocurrent (I_{ph}), diode saturation current (I_o), diode ideality factor (a), series ohmic resistance (R_s), and shunt ohmic resistance (R_p). The output current of the PV cell is presented in (1).

$$I = I_{ph} - I_o \left(\frac{(V+I \cdot R_s)}{aV_T} - 1 \right) - \left(\frac{V+I \cdot R_s}{R_p} \right) \quad (1)$$

$$V_T = k \cdot \frac{T_c}{q} \quad (2)$$

Where, V_T denotes the thermal voltage due to temperature dependency, k denotes the Boltzmann constant, q denotes the electron charge, T_c denotes the cell temperature, V denotes the PV cell voltage, and I denotes the PV cell current.

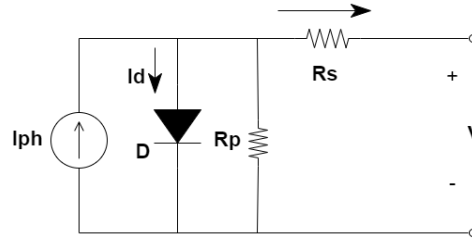


Figure 1. Equivalent linear diode solar cell model

2.1. Determination of I_{ph}

In standard testing conditions, the current output is as (3).

$$I = I_{ph,ref} - I_{o,ref} \left[\exp \left(\frac{V}{a_{ref}} \right) - 1 \right] \quad (3)$$

In (3) allows quantifying $I_{ph,ref}$ which cannot be decided differently. The short-circuit current of the PV cell is calculated using (4).

$$I_{sc,ref} = (I_{ph,ref} - I_{o,ref}) \left[\exp \left(\frac{V}{a_{ref}} \right) - 1 \right] = I_{ph,ref} \quad (4)$$

However, this equation is only applicable in the ideal situation. As a result, equality is incorrect. Then, in (4) must be written as (5).

$$I_{ph,ref} \approx I_{sc,ref} \quad (5)$$

The photocurrent is impacted by both irradiation and temperature, as presented in (6).

$$I_{ph} = \left(\frac{G}{G_{ref}} \right) (I_{ph,ref} + \mu_{sc} \cdot \Delta T) \quad (6)$$

Where, G signifies the solar irradiation $\frac{W}{m^2}$, G_{ref} denotes G at STC ($1000 \frac{W}{m^2}$), $\Delta T = T_c - T_{c,ref}$ (Kelvin), $T_{c,ref}$ denotes the cell temperature in $STC = 25 + 272 = 297$ K, I_{sc} denotes the short-circuit current, and $I_{ph,ref}$ denotes the photocurrent at STC.

2.2. Determination of I_o

The shunt resistance R_p is generally regarded as large, so the last term of the relationship should be ignored for the following approximation, By utilizing the three most notable points under typical test conditions: the open circuit voltage ($I=0$, $V = V_{oc,ref}$), the current during a short-circuit ($V=0$, $I = I_{sc,ref}$), as well as the voltage ($V_{mp,ref}$) and current ($I_{mp,ref}$) at MPP, the following relations are written [46].

$$I_{sc,ref} = (I_{ph,ref} - I_{o,ref}) \left[\exp \left(\frac{I_{sc,ref} \cdot R_s}{a_{ref}} \right) - 1 \right] \quad (7)$$

$$0 = I_{ph,ref} - I_{o,ref} \left[\exp \left(\frac{V_{oc}}{a_{ref}} \right) - 1 \right] \quad (8)$$

$$I_{pm,ref} = I_{ph,ref} - I_{o,ref} \left[\exp \left(\frac{V_{pm,ref} + I_{sc,ref} R_s}{a_{ref}} \right) - 1 \right] \quad (9)$$

After simplifications and assumptions, the following relations are obtained.

$$0 \approx I_{sc,ref} - I_{o,ref} \exp\left(\frac{V_{oc,ref}}{a_{ref}}\right) \quad (10)$$

$$I_{o,ref} = I_{sc,ref} \exp\left(\frac{-V_{oc,ref}}{a_{ref}}\right) \quad (11)$$

The reverse saturation current is stated as (12).

$$I_0 = DT^3 \exp\left(\frac{-q\varepsilon_G}{A \cdot K}\right) \quad (12)$$

Where, ε_G denotes material band-gap energy in eV, and D signifies the diode distribution coefficient.

2.3. Determination of R_p and R_s

To make the suggested model more reasonable, R_p and R_s are selected in such a way that the quantified maximum power P_{mp} is comparable to the experiment one $P_{mp,ex}$ at STC. As a result, the following equation can be written [46].

$$R_p = \frac{V_{mp,ref} + I_{mp,ref} R_s}{I_{sc,ref} - I_{sc,ref} \left\{ \exp\left[\frac{V_{mp,ref} + R_s I_{mp,ref} - V_{oc,ref}}{a}\right] + I_{sc,ref} \left\{ \exp\left[\frac{-V_{oc,ref}}{a}\right] - \left(\frac{P_{max,ex}}{V_{mp,ref}}\right) \right\} \right\}} \quad (13)$$

The repetition process begins at $R_s = 0$, which must rise to progress the MPP is getting closer to the experimental MPP. The corresponding R_p is then measured. There is just a single pairing available (R_p R_s). To show that the proposed paradigm is more reasonable, R_p and R_s are chosen in such a way that the computed maximal power P_{mp} is equivalent.

2.4. Short circuit current (I_{sc}) and open circuit voltage (V_{oc})

At normal sun irradiation levels, the short-circuit current is similar to the photocurrent I_{ph} , which is proportionate to the amount of solar energy G in $\frac{W}{m^2}$. The short-circuit current (I_{sc}) of the PV modules really aren't temperate-sensitive. It has the propensity to rise slightly when the module's temperature rises. This variance can be regarded as minor for modelling PV module performance. The short-circuit current I_{sc} can therefore be easily computed by employing the actual irritation condition.

$$I_{sc} = I_{sc} \left(\frac{G}{G_0}\right)^a \quad (14)$$

Where, I_{sc} signifies PV module short-circuit current under the normal solar intensity. The open-circuit voltage V_{oc} at any particular time and place can be represented as (15).

$$V_{oc} = \frac{V_{oc0}}{1+b\left(\frac{G_0}{G}\right)} \left(\frac{T_0}{T}\right)^c \quad (15)$$

Where, V_{oc} and V_{oc0} are the PV open-circuit voltages, G denotes average sun illumination, G_0 denotes the normal solar radiation, b denotes the PV module coefficient with no dimensions, c denotes the exponent considering all nonlinear effects of temperature, T denotes the PV module temperature considering normal sun illumination, and T_0 denotes actual temperature.

2.5. Impacts of bypass diodes in photovoltaic arrays

By forming a current channel around the defective cell, bypass diodes used in conjunction with either a single or a group of photovoltaic cells prevent current from passing from excellent, well-exposed to light, overheated PV cells and flaming out weak or partially shaded PV cells. Blocking diodes is not the same as power dissipation. Bypass diodes are often linked parallel to a PV cell or panels to shunt current around them while blocking diodes are typically connected series to the PV panels to keep current that passes from returning into existence. Blocking diodes differ from bypass diodes because, while the diode is physically the same in most circumstances, it is fitted separately and has a distinct purpose. Figure 2 shows the impact of the bypass diode on the I-V PV characteristics of two PV modules connected in series.

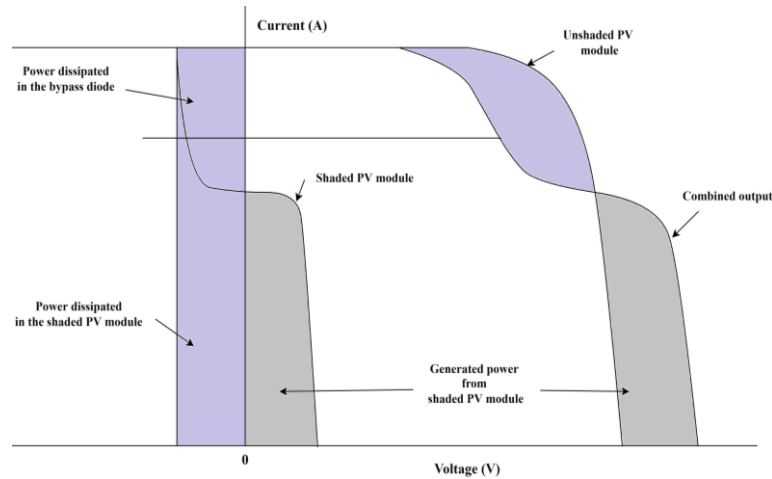


Figure 2. Impact of bypass diode on the PV characteristic of two PV modules connected in series

3. DC-DC POWER CONVERTER

The boost converter is employed in order to enhance the direct current voltage in compliance with the duty ratio derived based on the output voltage circumstance. The structure of the boost converter includes an inductor, switch, diode and capacitor. The outcome enhanced voltage surpasses the source voltage. The boost converter circuit is provided in Figure 3. The operational modes of the boost converter are as follows:

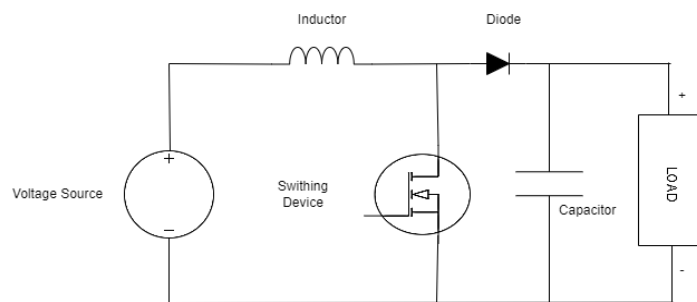


Figure 3. Circuit of boost converter

3.1. Mode 1 (MOSFET ON)

The equivalent functional circuit for mode 1 is provided in Figure 4. In this mode, the switching pulse is provided as high for the switch, and the inductor starts getting charged during this period. During Mode 1, the capacitor keeps the output voltage at the desired level. The inductor voltage and output boosted voltage are given as:

$$V_L = V_{in} \quad (16)$$

$$V_{Co} = V_o \quad (17)$$

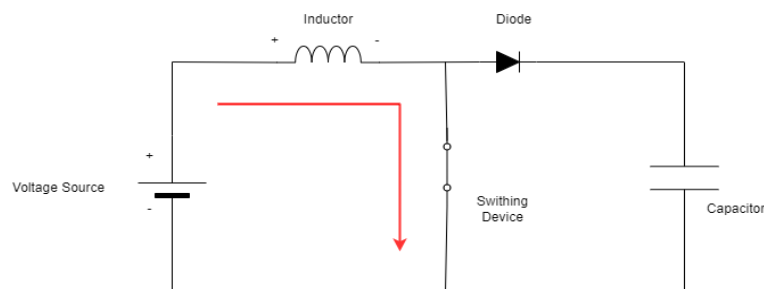


Figure 4. Mode 1: equivalent circuit of boost converter, $V_L=V_{in}$

3.2. Mode 2 (MOSFET OFF)

The identical operational circuit for Mode 2 is provided in Figure 5. In this mode, the switching pulse is provided as low for the switch, and the inductor starts getting discharged during this period. The inductor voltage and output boosted voltage are given as (18).

$$V_o = V_L + V_{in} \quad (18)$$

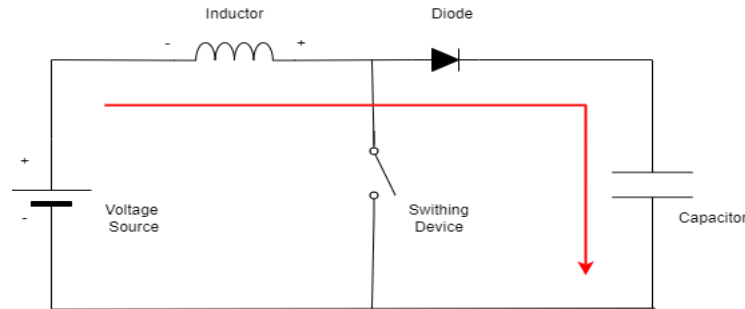


Figure 5. Mode 2: equivalent circuit of boost converter, $V_o = V_{in} + V_L$

The boost converter design equations are given as follows. The pulse width (D) of the boost converter is provided in (19).

$$D = \frac{V_o}{V_o - V_{in}} \quad (19)$$

The inductance is designed according to in (20).

$$L = \frac{V_{in} * D}{\Delta I_o * F_{sw}} \quad (20)$$

The ripple current allowed across the inductor is provided in (21).

$$\Delta I_L = 0.2 * \frac{V_o}{V_{in}} * I_o \quad (21)$$

The output side capacitance value is calculated using in (22).

$$C_o = \frac{I_o * D}{F_{sw} * \Delta V_o} \quad (22)$$

The ripple voltage allowed across the output side capacitance is provided in (23).

$$\Delta V_o = 2\% \text{ of } V_o \quad (23)$$

4. MAXIMUM POWER POINT TRACKING ALGORITHMS

In this study, 4 different algorithms are discussed, which include two classical algorithms, such as P&O and INC and two modern optimization algorithms, such as MVP and ARO.

4.1. Most valuable player algorithm

MVP algorithm is a type of metaheuristic algorithm which explores and exploits the solution, similar to other search-based stochastic algorithms [40]. The performance of the players (solutions) depends on individual skills, which resemble the dimensions of the optimization problem. The competition among players in a single team leads to the franchise player of a team, and competition among teams leads to the most valuable player (optimal solution). The individual player with various skill sets is provided in (24).

$$player_1 = [Skill_1, Skill_2, Skill_3 \dots Skill_z] \quad (24)$$

Where z is the number of the dimensions and $Skill_1, Skill_2, Skill_3 \dots Skill_z$ are the skills of the l^{th} player. The v^{th} team, which consists of several players, is mentioned in (25).

$$Team_v = [player_1, player_2, player_3, \dots, player_{ps}] \quad (25)$$

Where, ps is the number of players for team v , and the v^{th} team is provided in (26) by combining (24) and (25).

$$Team_v [Skill_{11}, Skill_{1z}, Skill_{21}, Skill_{2z}, Skill_{31}, Skill_{3z}, Skill_{ps1}, Skill_{psz}] \quad (26)$$

The squad size is based on the number of athletes and is chosen randomly so that the team size might be uneven. The team is formed as provided in the following steps: the teams are classified into mT_1 and mT_2 teams. The mP_1 (27) players are placed in mT_1 (29) and mP_2 (28) players are placed in mT_2 (30).

$$mP_1 = \text{ceil} \left(\frac{\text{player Size}}{\text{Teams Size}} \right) \quad (27)$$

$$mP_2 = mP_1 - 1 \quad (28)$$

$$mT_1 = \text{PlayersSize} - mP_2 \times \text{TeamsSize} \quad (29)$$

$$mT_2 = \text{TeamsSize} - mT_1 \quad (30)$$

Where, PlayersSize is the number of participants, and TeamsSize is the total number of teams within a given tournament. The round-off function makes it an integer to the minimum value of the following integers. The tournament is started after the teams are formed.

4.1.1. Individual competition

The single-team players compete among themselves to select a franchise player. The player's skill or duty ratio is updated in (31).

$$Team_v = Team_v + \text{rand} \times (\text{Franchise}_v - Team_v) + 1.2 \times \text{rand} \times (\text{MVP} - Team_v) \quad (31)$$

Where, Franchise_v is the most valuable player on v th team, MVP is by far the most valuable player in the entire competition, $Team_v$ is the skill of a specific player among team v participants, and rand will be termed as a random variable.

4.1.2. Team competition

Here, various teams compete in the tournament, and at any given contest, one team competes with the other; at the end, any team wins, and the fitness values are updated after the match. The normalized fitness equation for a particular team is provided in (32).

$$\text{fit}(Team_v) = \text{fit}(Team_v) - \text{minimum}(\text{fit}(\text{AllTeams})) \quad (32)$$

The following equation provides the possibility of an outcome for any match.

$$\text{Prob}\{\text{Team}_j \text{ Beat Team}_k\} = 1 - (\text{fit}_N(\text{Team}_j))^p + (\text{fit}_N(\text{Team}_j))^p + (\text{fit}_N(\text{Team}_k))^p \quad (33)$$

If $\text{Prob}\{\text{Team}_j \text{ Beat Team}_k\}$ is higher than that of $\text{Prob}\{\text{Team}_k \text{ Beats Team}_j\}$ it means Team j wins. A reality factor is added to the equation mentioned above as, in real-time, the results vary even at the last moment; hence, a random variable is combined with the probability equation. If the random number is higher than 0.5, $team_j$ wins if not the $team_k$ wins and the players' skills in the competing teams are updated by (34) and (35) based on win or lose.

$$Team_j = Team_j + \text{rand} \times (Team_j - \text{Franchise}_k) \quad (34)$$

Otherwise:

$$Team_j = Team_j + \text{rand} \times (\text{Franchise}_k - Team_j) \quad (35)$$

after that, the greediness function is applied, where the fitness values of players before and after the tournament starts are compared, and higher values are adapted. If two players possess the same order of skills, then one player is replaced. The worst players are replaced with the best players' best solutions, and the

execution of the algorithm is terminated if the given criterion is fulfilled. The flowchart of the MVP algorithm is provided in Figure 6.

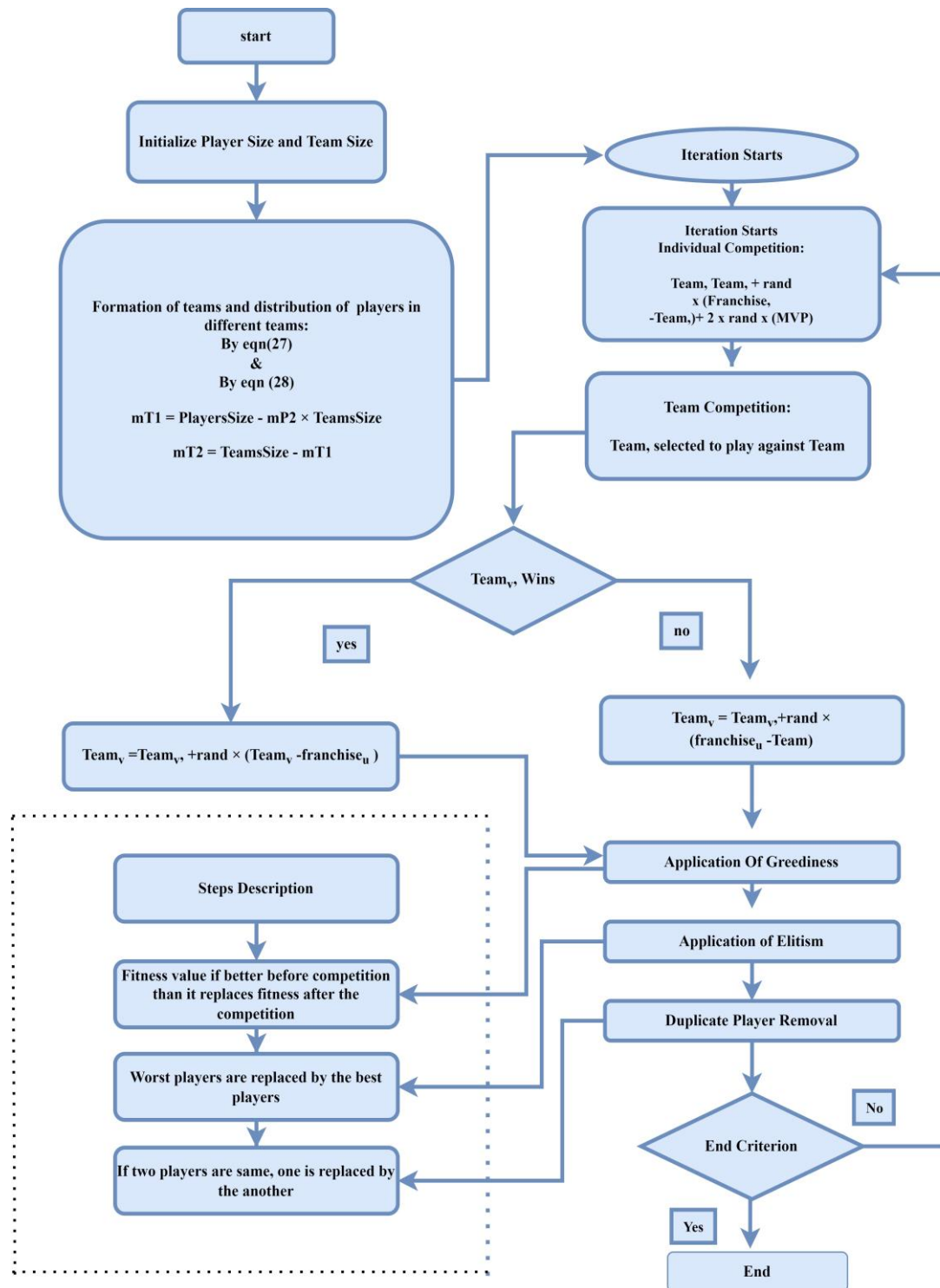


Figure 6. MVP algorithm flowchart

4.2. Artificial rabbit optimization algorithm

Artificial rabbit optimization (ARO) is a unique biologically-inspired method that has been developed, and this algorithm is designed to give a solution for single-objective global optimization problems [45]. The artificial rabbit optimization algorithm is inspired by the rabbit's survivability tactics and is carefully

explored and quantitatively modelled. This algorithm is comprised of three searching modes first is detour foraging tactics, random hiding tactics, and energy shrink tactics come in the last. The detour foraging strategy gives credits to exploration; the random hiding strategy is devoted to utilization; and the power reduction method strengthens the balance between exploitation and exploration. ARO is used to extract maximum power from the photo voltaic module in typical circumstances, and various settings of intermittency provides the searching and hiding techniques of real rabbits and the energy shrink, which causes a transition between the techniques mentioned above.

4.2.1. Detour foraging

The rabbits each have their own grazing area, but it randomly consumes the grass in other areas and tends to perturb around the food source, which provides information about the position of other individual rabbits. This behavior is used in MPPT where the duty ratio denotes the rabbit, and it randomly checks for other duty ratios and hence updates the position of other local power peaks. As mentioned below, the mathematical model is proposed for the ARO algorithm's detour foraging step.

$$\vec{v}_i(t+1) = \vec{x}_j(t) + R * (\vec{x}_i(t) - \vec{x}_j(t)) + \text{round}(0.5 * (0.05 + r_1)) * n_1 \quad (36)$$

$$R = l * c \quad (37)$$

$$l = (e - e^{\left(\frac{t-1}{T_{max}}\right)^2}) * \sin(2\pi r_2) \quad (38)$$

$$c \cdot (k) = \begin{cases} 1 & \text{if } k == G(l) \\ 0 & \text{else} \end{cases} \quad l \cdot k = 1, \dots, d \quad \text{and } l = 1, \dots, (r_3 \cdot d) \quad (39)$$

$$g = \text{randp}(d) \quad (40)$$

$$n_1 \sim (0, 1) \quad (41)$$

Where, $\vec{v}_i(t+1)$ is the position of i^{th} duty ratio at the time $(t+1)$, $\vec{x}_i(t)$ is the position of i^{th} duty ratio at time t , n is the number panels, d signifies the dimensions, T denotes the highest iteration, $\lceil \cdot \rceil$ denotes the ceiling function which provides next possible integer, round denotes nearest possible integer, randperm allows for the random shuffling of numerals spanning 1 to d , r_1 , r_2 , and r_3 are the random variables with the range of $(0,1)$, L is the change in duty ratio or the gap to perform random, and n_1 is normalized standard distribution. This guarantees the capability for a global range of searches of the ARO algorithm.

4.2.2. Random hide

The rabbit usually built various burrows for hiding purposes, and in this algorithm, for each iteration, a position of duty ratio is generated, and the current position is randomly chosen among the generated duty ratios. The j^{th} the tunnel of i^{th} rabbit gets delivered as:

$$\vec{b}_i(t) = \vec{x}_i(t) + H * g * \vec{x}_i(t), i = 1, \dots, n \text{ and } j = 1, \dots, \partial M \quad (42)$$

$$H = (T - t + 1)T * r_4 \quad (43)$$

$$n_2 \sim (0, 1) \quad (44)$$

$$g(k) = \begin{cases} 1 & \text{if } k == j \\ 0 & \text{else} \end{cases} \quad l * k = 1, \dots, d \quad (45)$$

From (42), the d number of duty ratios is generated nearby to the original position of duty ratio. H is linearly decreased from 1 to l/T_{max} with several perturbations randomly for the total amount of repetitions in complete. The range of the generated duty ratios is reduced around the global peak of power as the iterations proceed gradually. The mathematical equations for the above-mentioned random hiding technique are provided as:

$$\vec{v}_i(t+1) = \vec{x}_i(t) + R * (r_4 * \vec{b}_i(t) - \vec{x}_i(t)), \quad (46)$$

$$gr(k) = \begin{cases} 1 & \text{if } k == \lceil r_5 \cdot d \rceil \\ 0 & \text{else} \end{cases} \quad l * k = 1, \dots, d \quad (47)$$

$$\vec{b}_i(t) = \vec{x}_i(t) + H * gr * \vec{x}_i(t) \quad (48)$$

Where, \vec{b}_i and γ provides the random locations of duty ratios and, r_4 and r_5 are two randomized factors with readings inside a certain limit of (0,1). As per in (46), the i^{th} search duty ratio updates its positioning about the randomly chosen place out of its original position. The rabbit or duty ratio position is updated once detour hunting and haphazard concealing process are attained.

$$\vec{x}_i(t+1) = \begin{cases} \vec{x}_i(t) & \text{if } f(\vec{x}_i(t)) \leq f(\vec{v}_i(t+1)) \\ \vec{v}_i(t+1) & \text{else } f(\vec{x}_i(t)) > f(\vec{v}_i(t+1)) \end{cases} \quad (49)$$

4.2.3. Energy shrink

In initial iterations, the ARO undergoes the detour foraging phase and searches for the local peaks, and in final iterations, random hiding is performed in which the current duty ratios shift around the global peak and update the positions. The transfer of phases is termed as energy shrinks as a source of energy to simulate the ARO switching process from the preliminary investigation to the defined stage. The power element is provided in (50).

$$A(t) = 4 * \left(1 - \frac{t}{T_{max}}\right) * \ln * \frac{1}{r} \quad (50)$$

Where, r is indeed the random variable whose range is within (0,1). All the update processes and computations are done until the end condition is satisfied and the best possible solution is retrieved. The pseudocode of ARO is presented in *algorithm*. The flowchart of ARO is shown in Figure 7.

4.3. Incremental conductance (INC) method

The INC algorithm detects the slope of the P-V curve, and the MPP is tracked by searching the peak of the P-V curve. This algorithm uses the instantaneous conductance $\frac{I}{V}$ and the incremental conductance $\frac{\Delta I}{\Delta V}$ for MPPT. Depending on the relationship between the two values, as expressed in (55)-(57), the location of the PV module's operating point in the P-V curve can be determined, i.e., in (55) indicates that the PV module operates at the MPP, whereas (56)-(57) indicate that the PV module operates on the left and right sides of the MPP, respectively, in the P-V curve.

$$\frac{dP}{dV} = 0 \quad \text{at MPP} \quad (51)$$

$$\frac{dP}{dV} > 0 \quad \text{left of MPP} \quad (52)$$

$$\frac{dP}{dV} < 0 \quad \text{right of MPP} \quad (53)$$

$$\frac{dP}{dV} = \frac{d(VI)}{d(V)} = I + V * \frac{dI}{dV} \quad (54)$$

The maximum power point identifier factor is defined as $\frac{dP}{dV}$. The INC approach has proposed accurately monitoring a PV array's MPP by leveraging this component. To track the MPP, the following definitions are used.

$$\frac{\Delta I}{\Delta V} = \frac{-I}{V} \quad (55)$$

$$\frac{\Delta I}{\Delta V} > \frac{-I}{V} \quad \text{left of MPP, } \Delta V_n = +\delta \quad (56)$$

$$\frac{\Delta I}{\Delta V} < \frac{-I}{V} \quad \text{right of MPP, } \Delta V_n = -\delta \quad (57)$$

The MPPT controls until the DC/DC converter energy converter's pulse width modulation (PWM) signal following condition is met: $(\frac{dP}{dV}) + (\frac{-I}{V}) = 0$ is delivered. Take the n^{th} repetition of the method as a starting point, and then use the equations above to calculate the $n+1$ iteration process. The output signal of the INC method is used to change the voltage reference of the PV array with only an increased or decreased constant value (V) in relation to the second common voltage. Regardless of the distance between the set's PV and MPP intersection region, this methodology tracks MPP with a fixed step size. Figure 8 depicts the flowchart of incremental conductance-based MPPT.

Algorithm: Pseudocode of ARO algorithm

- Step 1: The dimensions of artificial rabbits optimization, including the size of artificial rabbits N , and T_{max} .
- Step 2: Instantiating a rabbit collection at random z_i and compute f_i
- Step 3: Find the finest rabbit.
- Step 4: While $t \leq T_{max}$. do
 - For $i = 1$ to N , do
 - Compute the energy element
 - If $A > 1$ then
 - Randomly choose rabbits from all individuals.
 - Compute R
 - Use the detour hunting approach.
 - Determine the rabbit's position's optimal solution.
 - The positioning of a rabbit has been revised.
 - Else
 - Generate d burrows and select one randomly
 - Use a randomized concealment approach.
 - Determine the rabbit's position's optimal solution f_i
 - The positioning of a rabbit has been revised.
 - End if
 - End for
 - Check for the finest artificial rabbit.
 - $t = t + 1$.
 - End while
- Step 5: Determine the best artificial rabbit.

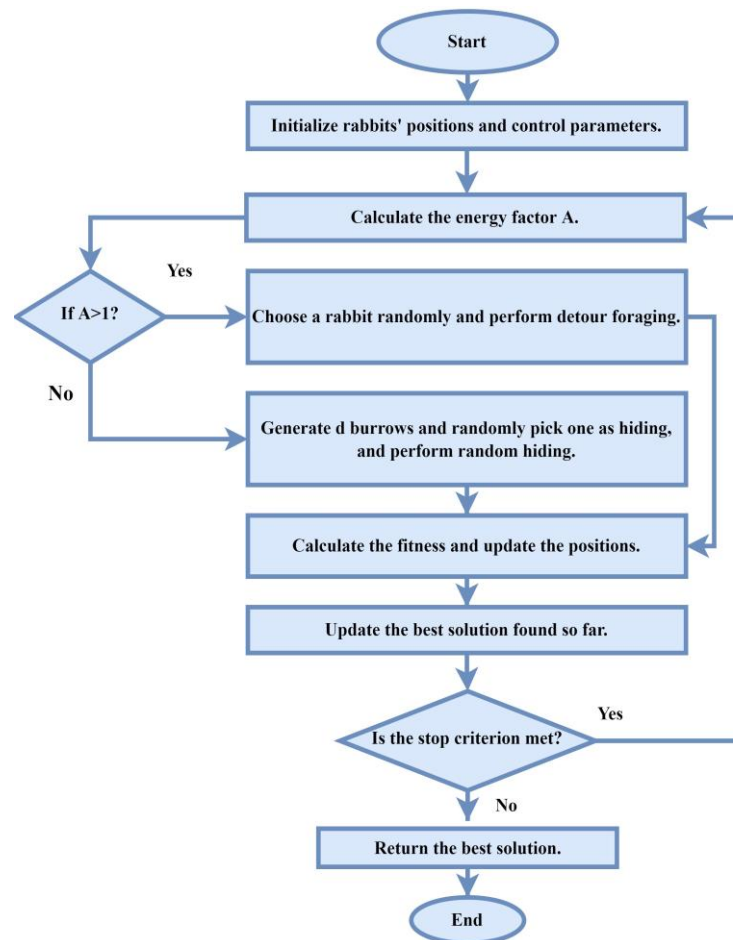


Figure 7. ARO algorithm flowchart

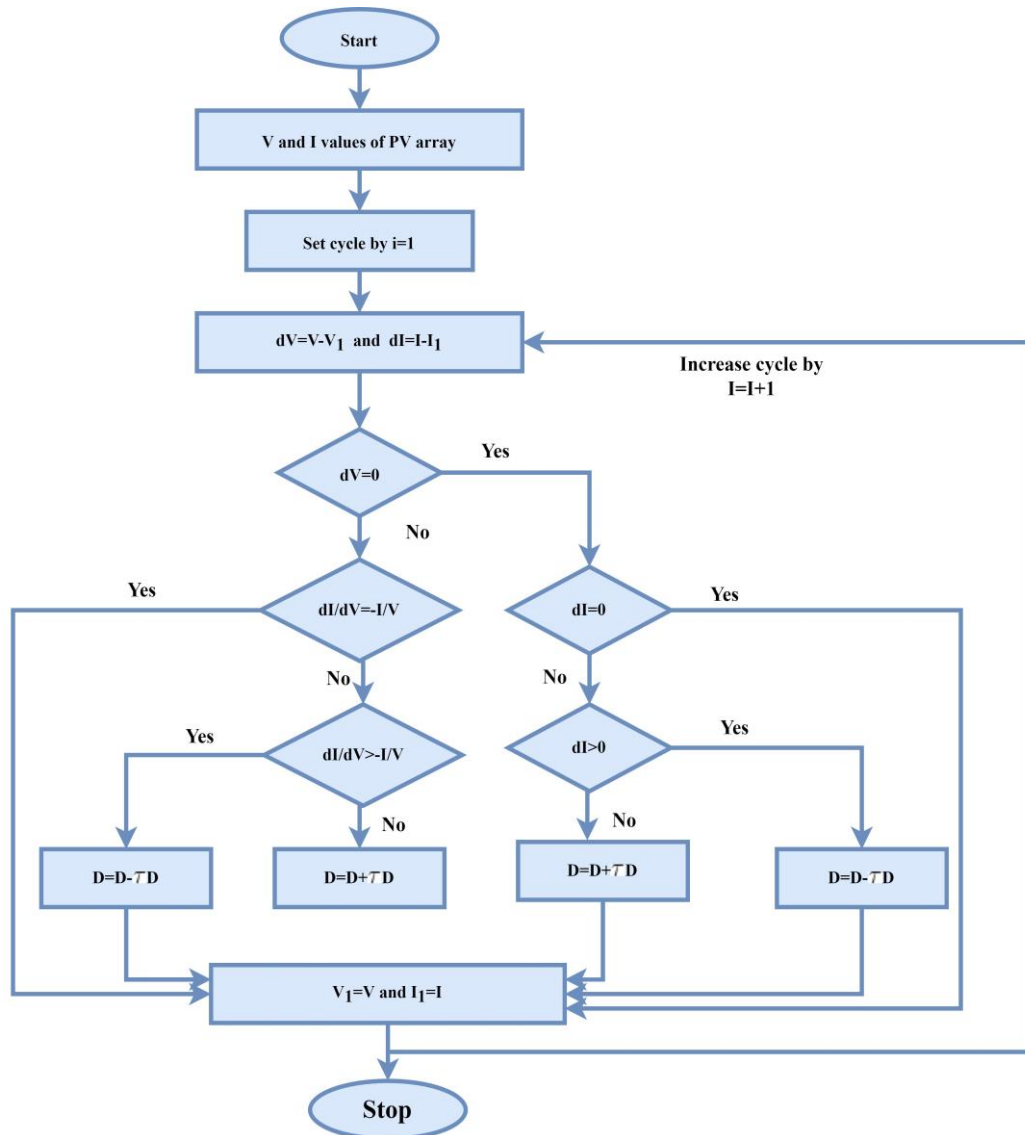


Figure 8. Flowchart of the INC algorithm

4.4. Perturb and observe algorithm (P&O)

The P&O algorithm detects and extracts the most power from the PV system. In this case, the photovoltaic voltage is only slightly perturbed, and the power P is evaluated. If P is positive, the PV voltage perturbation approaches towards the maximum power point. The outcome is that the perturbation is continued until P reaches the +ve zone. If P is negative, the PV voltage perturbation is pushed closer to MPP, and the Instability's orientation is inverted for MPP to be impacted by power.

$$\text{If } \frac{\Delta P}{\Delta V} > 0, \Delta D \text{ is } +ve, \quad (58)$$

$$\text{If } \frac{\Delta P}{\Delta V} < 0, \Delta D \text{ is } -ve. \quad (59)$$

Variables like dI and dV are +ve; hence, the increase in solar irradiation can also be recognized by an additional variable, dI . Hence, the duty ratio is modified in such a manner to minimize the operating voltage, in which dI and dV are +ve and avoid the control issue by modifying the switching indicated towards the direction of MPP. Figure 9 depicts a flowchart of the P&O algorithm-based MPPT.

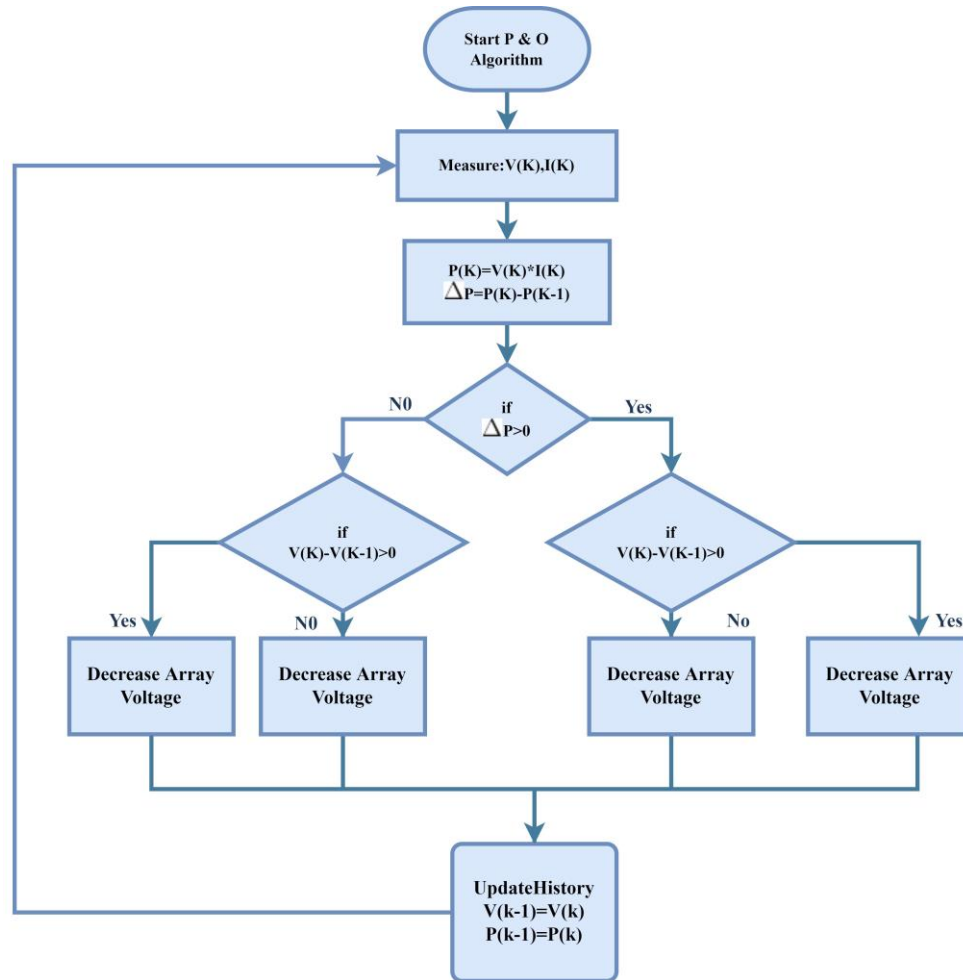


Figure 9. Flowchart of the P&O algorithm

5. SIMULATION RESULTS AND DISCUSSIONS

Figure 10 shows the Simulink model of a PV system, where the extensively utilized DC-DC boost converter is developed and used for simulating and comparing all four algorithms for various testing conditions like standard testing, one-step iteration, and rapid testing. We have used PV arrays to change irradiance by shifting 4S configuration instances. The PWM generator generates a pulse and sends it to the boost converter. The proposed algorithms are introduced with the boost converter, and the result of the PV model is seen in scope.

The MVP and ARO algorithms are tested on several PV configurations by contrasting the simulation data achieved by the classical algorithms, such as the P&O and INC algorithms. The suggested technique is built and evaluated using a typical boost converter under diverse insolation and partially shaded circumstances. The testing scenarios are shown in Table 1. Each shade pattern lasts 2 seconds, and many other factors determine the computation time. The algorithm parameters for all techniques are kept constant to evaluate the proposed methods' effectiveness.

Table 1. Various shading patterns on four modules

Condition	Instance	Irradiance (W/m2)				Temperature
		Panel1	Panel2	Panel3	Panel4	
Standard	1	1000	1000	1000	1000	[25,25,25,25]
	1	1000	650	520	300	[25,25,25,25]
	2	1000	850	650	480	[25,25,25,25]
	3	1000	950	800	650	[25,25,25,25]
	4	1000	1000	640	450	[25,25,25,25]
	5	1000	1000	1000	720	[25,25,25,25]
One step	6	1000	1000	1000	1000	[25,25,25,25]
	1	1000	850	650	480	[25,25,25,25]
	2	1000	950	800	650	[25,25,25,25]

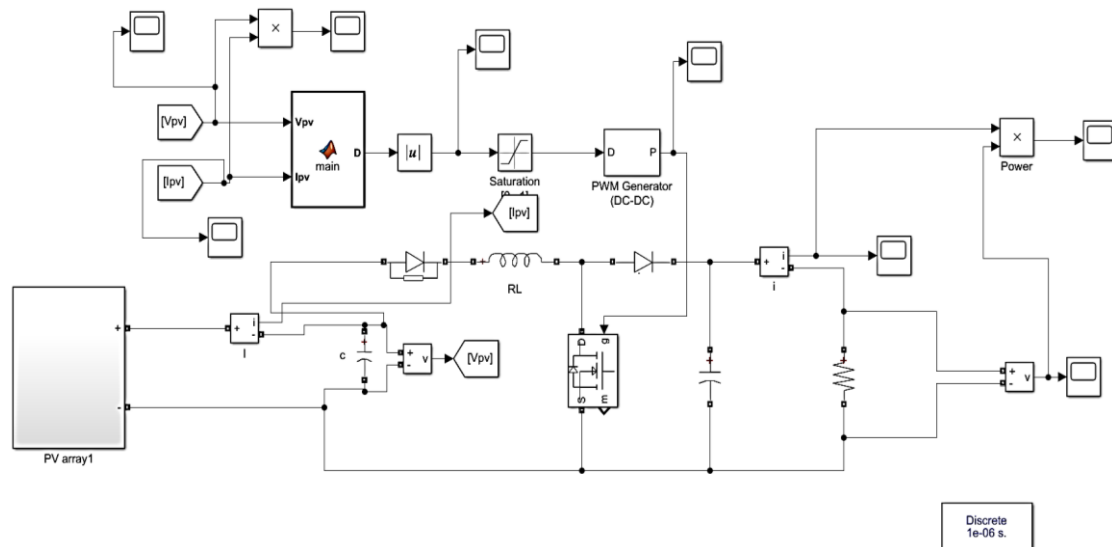


Figure 10. Simulink model of PV system

MATLAB/Simulink version 2018b is used to Simulate the specified photovoltaic system on a laptop with an Intel Core i5 AMD Ryzen 7 5800H with NVIDIA GeForce RTX Graphics 3.20 GHz and RAM of 16 giga bytes. In MATLAB, the solver is Dormand-Prince (ode45), and the scaling factor is configured to vary automatically. ARO's result is evaluated alongside other algorithms such as MVP, P&O, and INC. The number of repetitions and population size are critical metaheuristic algorithm constants. Therefore, these two variables were optimized based on the results of several trials and the information from the research.

5.1. Standard testing condition

The initial insolation is preserved at 1000 W/m^2 with a constant temperature of 25°C . The comparison is made between MVP, ARO algorithms and classical algorithms like P&O and INC for the standard testing condition results. The maximum power extracted by the MVP-based MPPT methodology is around 86.25 W, with an effectiveness of 98.74% and a tracking time of 0.48 seconds. Maximum power extracted by the ARO-based MPPT algorithm is around 86.8 W with an efficiency of 99.37% Using a 0.03 tracking time (s). Maximum power extracted by the P&O-based MPPT algorithm is around 78.6 W with an efficiency of 89.98% with a tracking time of 0.03 seconds, and maximum power extracted by the INC-based MPPT algorithm is around 69.02 W with an efficiency of 79.01% with the tracking time of 0.016 seconds when every panel is subjected to no shading conditions. INC can track the maximum duty cycle at 0.016 seconds and settle down to constant voltage at 0.02 seconds, P&O can track the maximum duty cycle at 0.016 seconds and settle down to constant voltage at 0.02 second, MVP can track maximum duty cycle 0.8 at 0.02 seconds and settle down to constant duty cycle at 0.48 second, ARO algorithm can track maximum duty cycle 0.25 at 0.015 seconds and settle down to constant duty cycle at 0.02 seconds. Figure 11 shows that the ARO algorithm can track better effectiveness in standard testing conditions than other algorithms. Figure 11 gives the standard testing conditions results of all four algorithms. Figure 11(a) shows the PV output power, Figure 11(b) shows the PV output voltage, Figure 11(c) shows the PV output current, and Figure 11(d) shows the comparison of the duty cycle of all four algorithms.

5.2. One-step irradiance condition

The initial solar insolation is preserved at 745 W/m^2 in the first instance and then increased to 850 W/m^2 in the second instance after 2 seconds. Figure 12 shows that the MVP algorithm can find the MPP at 60.93 W with 93.03% efficiency during the first two seconds of the first interval and at 41.78 W with 56.26% efficiency during the second two seconds of the second interval. The ARO algorithm can locate the MPP at 31.65 W with 48.3% efficiency during the first 2 seconds and 32.4 W with 43.32% efficiency during the second 2 seconds. The INC algorithm can locate the MPP at 23.71 W with 36.41% effectiveness during 0–2 seconds in the first interval and 32.37 W with 43.26% efficiency during 2–4 seconds in the second interval. The P&O technology locates the MPP at 39 W with 58.58 percent efficiency during the first 2 seconds and 50.1 W with 67.46% efficiency during the second 2 seconds. Figure 12 gives the one-step irradiance condition results of all four algorithms. Figure 12(a) shows the PV output power, Figure 12(b) shows the PV output voltage, Figure 12(c) shows the PV output current, and Figure 12(d) shows the comparison of the duty cycle of all four algorithms.

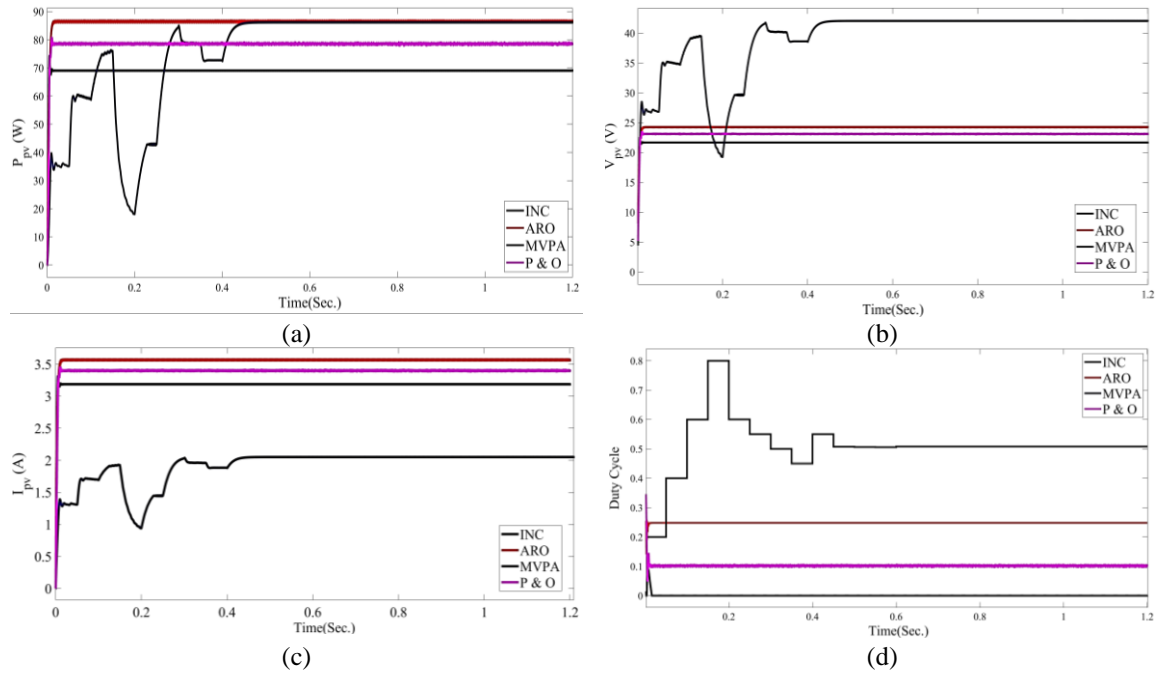


Figure 11. Simulation waveforms under standard testing conditions (a) PV power, (b) PV voltage, (c) PV current, and (d) duty cycle

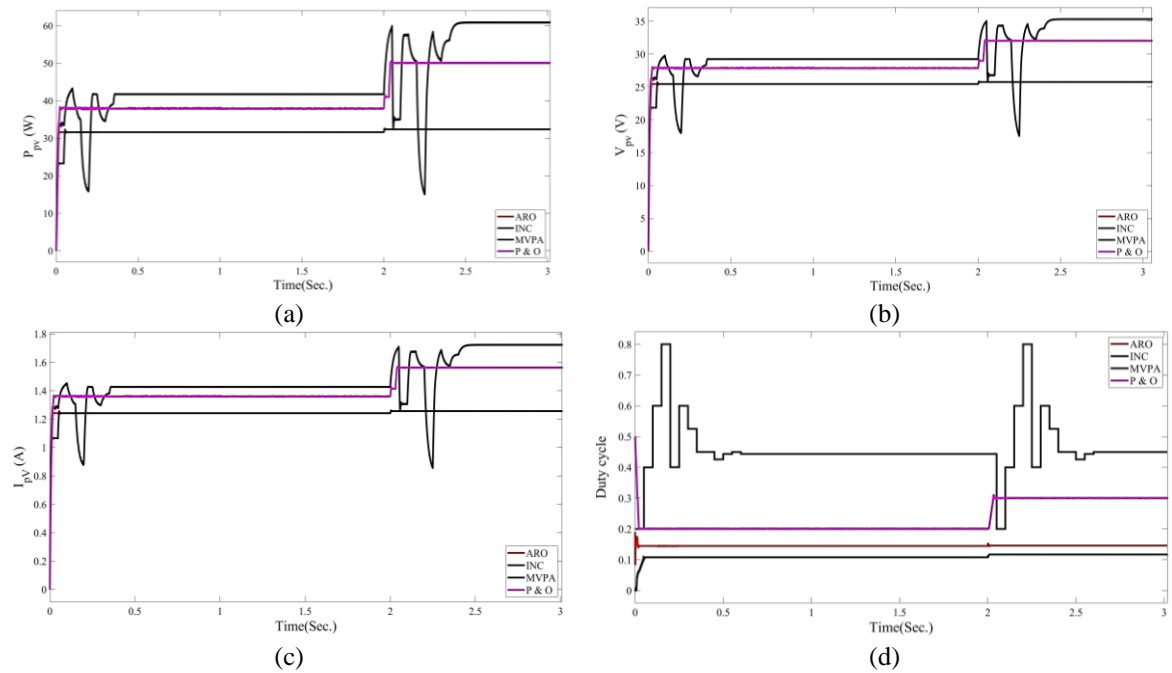


Figure 12. Simulation waveforms under one-step change of irradiances (a) PV power, (b) PV voltage, (c) PV current, and (d) duty cycle

5.3. Rapid testing conditions

Solar irradiance changes quite drastically during overcast periods of the season, impacting the effectiveness of PV systems. A study presented characterized a rapid change in solar irradiance as also being considered to boost the effectiveness of the offered techniques. As a result, the recommended algorithms are evaluated under rapid increases in radiation exposure. The simulation lasted for 12 seconds with six intervals of 2 seconds each, with the sun's insolation changing dramatically every 2 seconds. Figure 13 gives the rapid testing condition results of all four algorithms. Figure 13(a) shows the PV output power, Figure 13(b) shows

the PV output voltage, Figure 13(c) shows the PV output current, and Figure 13(d) shows the comparison of the duty cycle of all four algorithms. Figure 13 shows that the simulation began with 817 W/m^2 during 0–0.2 seconds in the first interval, then changed to 742 W/m^2 during 0.2–0.4 seconds in the second interval, 900 W/m^2 during 0.4–0.6 seconds in the third interval, 520 W/m^2 during 0.6–0.8 seconds for the fourth interval, 930 W/m^2 during 0.8–1 second for the fifth interval, and 1000 W/m^2 during the last instance. The simulation results shown in Figure 13 shows that the MVP method functions very well during an extreme shift in insolation. It is stated that the MVP algorithm can track the MPP at 41.8 W with 56% efficiency from 0 to 2 seconds in the first interval, 60.9 W with 93.64% efficiency in the second interval from 2 to 4 seconds, and 37.6 W with 70.90% efficiency in the third interval from 4 to 6 seconds. 41.8 W with 56% efficiency from 6 to 8 seconds in the fourth interval; 60.9W with 93.64% efficiency in the fifth interval from 8 to 10 seconds; and 37.6 W with 70.90% efficiency in the last interval from 10 to 12 seconds.

It has also been observed that classic P&O and INC algorithms fail to monitor the MPP effectively continuously, and the algorithms slip into the zone under rapid changes in irradiation. According to the results of numerous simulations, variable step size in conventional MPPT techniques and the ARO algorithm cannot increase tracking speed, accuracy, or efficiency during an extreme shift in insolation as much as the MVP algorithm tracks.

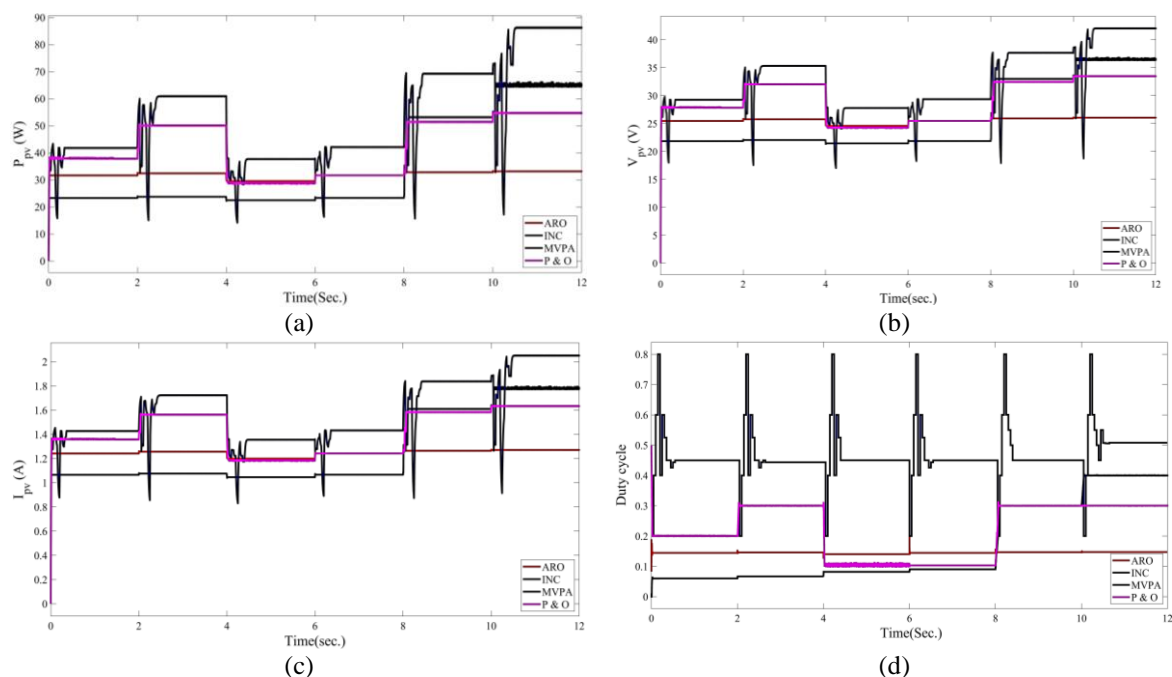


Figure 13. Simulation waveforms under rapid change of irradiances (a) PV power, (b) PV voltage, (c) PV current, and (d) duty cycle

5.4. Performance comparison

Table 2 gives the detailed performance of all four algorithms when algorithms are proposed under standard testing conditions. As tabulated, the MVP algorithm locates MPP at 86.25 W with 98.74% efficiency, whereas the ARO algorithm locates MPP at 86.83 W with an efficiency of 99.37% and classical algorithms such as P&O and INC tracks MPP at 69.02 W and 78.6 W respectively with an efficiency of 79.01% and 89.98%, hence considering these performance results of all four algorithms, we suggest that the ARO algorithm performs better in standard testing conditions. Figure 14 shows a pictorial representation of the comparison.

Table 2. Performance comparison: Case 1

Algorithms	Calculated power (W)	Extracted power (W)	% efficiency (%)	Tracking time (s)
MVP	87.35	86.25	98.74	0.48
ARO	87.35	86.83	99.37	0.03
INC	87.35	69.02	79.01	0.03
P & O	87.35	78.6	89.98	0.016

Table 3 gives the detailed performance of all four algorithms when proposed under one-step irradiance testing conditions. As evaluated in Table 3, the MVP algorithm locates MPP at 60.93 W in the first instance and 41.78 W in the second interval, with 93.03% and 56.26% efficiency, respectively. At the same time, the ARO algorithm can find MPP at 31.65 W in the first interval and 32.4W in the second interval with efficiencies of 48.66% and 43.32%, respectively. Classical algorithms such as INC track MPP at 23.71 W in the first instance and 38.312 W in the second interval, respectively, with efficiencies of 36.41% and 43.74%. The P&O algorithm locates MPP at 38.312 W in the first instance and 50.1 W in the second interval, with an efficiency of 58.58% and 67.47%. Hence, considering the performance results of all four algorithms, we suggest that the MVP algorithm performs better in one-step iteration testing conditions. Figure 15 shows a pictorial representation of the comparison (Case 2).

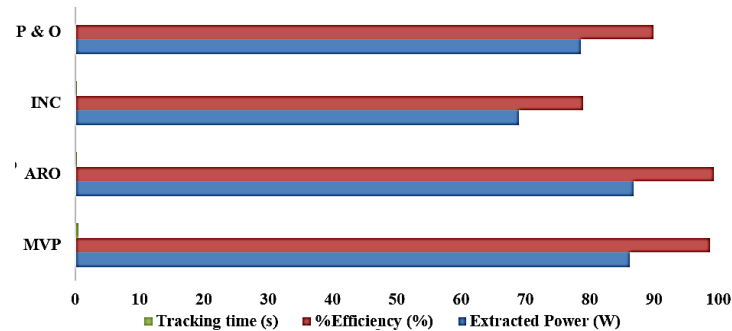


Figure 14. Pictorial representation performance metrics for Case 1

Table 3. Performance comparison: Case 2

Algorithms	Calculated Power (W)	Extracted Power (W)	%Efficiency (%)	Tracking time (s)
MVP	65.03	60.93	93.03	2.55
	74.25	41.78	56.26	0.38
ARO	65.03	31.65	48.66	0.03
	74.25	32.4	43.32	2.032
INC	65.03	23.71	36.41	2.03
	74.25	32.37	43.74	5.70
P&O	65.03	38.312	58.58	0.05
	74.25	50.1	67.47	2.05

Table 4 gives the detailed performance of all four algorithms when algorithms are proposed under rapid iteration testing conditions. As tabulated in Table 4, the MVP algorithm locates MPP at an average of 78.23% efficiency under rapid irradiance change. At the same time, the ARO algorithm locates MPP at an average of 69.55% efficiency, and classical algorithms such as P&O and INC track MPP at an average of 43.87% and 47.69% efficiency, respectively. From Table 4, it is evident that the ARO algorithm and classical algorithms fail to track better efficiency, whereas the MVP algorithm is slightly better in terms of efficiency under severe shading conditions. Figure 16 shows a pictorial representation of the comparison (Case 3).

Table 4. Performance comparison: Case 3

Algorithms	Parameters	Instances						Average Efficiency
		1	2	3	4	5	6	
MVP	Calculated Power (W)	74.25	65.03	53.03	67.48	79.05	87.35	78.23%
	Extracted Power (W)	41.81	60.9	37.6	42.02	69.2	86.3	
	%Efficiency (%)	56.30	93.64	70.90	62.27	87.53	98.79	
	Tracking time (s)	0.37	2.52	4.46	6.37	8.5	10.55	
ARO	Calculated Power (W)	74.25	65.03	53.03	67.48	79.05	87.35	69.55%
	Extracted Power (W)	31.65	32.4	29.5	31.64	32.8	33.04	
	%Efficiency (%)	42.65	49.82	55.62	47.22	41.49	37.97	
	Tracking time (s)	0.04	2.03	4.02	6.03	8.12	10.02	
INC	Calculated Power (W)	74.25	65.03	53.03	67.48	79.05	87.35	47.69%
	Extracted Power (W)	23.27	23.72	22.42	23.30	53.10	65.0	
	%Efficiency (%)	31.34	36.47	42.27	34.52	67.17	74.41	
	Tracking time (s)	0.04	2.03	4.02	6.03	8.12	10.03	
P&O	Calculated Power (W)	74.25	65.03	53.03	67.48	79.05	87.35	43.87%
	Extracted Power (W)	38.0	50.01	28.7	31.65	52.4	54.6	
	%Efficiency (%)	51.17	77.07	54.01	47.23	66.28	62.50	
	Tracking time (s)	0.04	2.06	4.12	6.02	8.03	10.02	

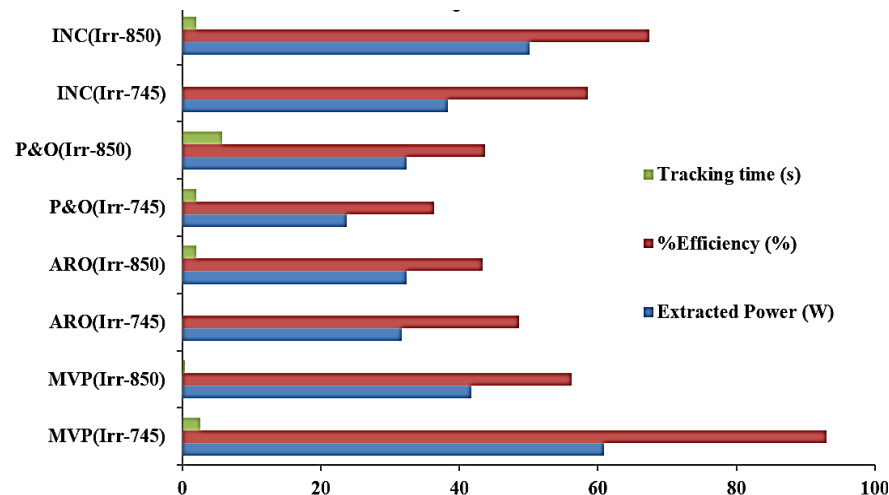


Figure 15. Pictorial representation performance metrics for Case 2

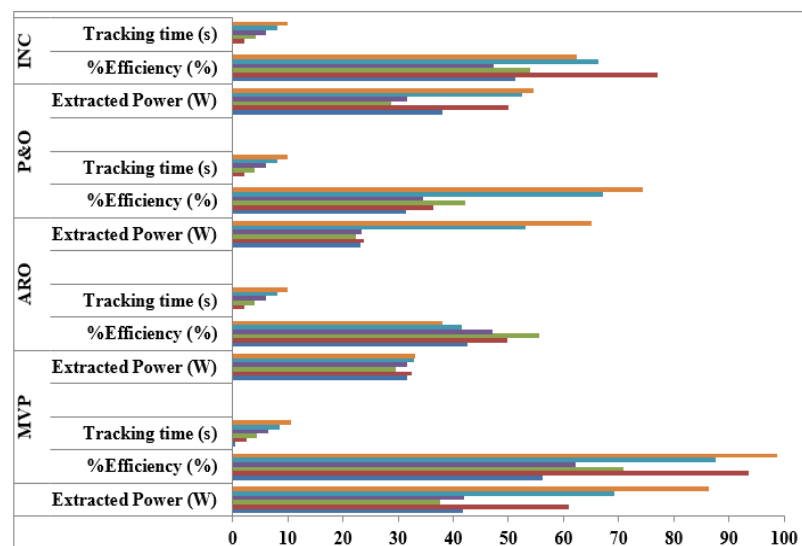


Figure 15. Pictorial representation performance metrics for Case 3

6. CONCLUSION

This study uses an extensive comparative analysis by considering recently reported metaheuristic algorithms, such as MVP algorithm and ARO for MPPT of PV systems. PV system with boost converter was subjected to recently proposed algorithms like MVP algorithm, and ARO algorithm is compared with classical algorithms like INC and P&O based techniques under various testing circumstances, such as standard testing method, one-step iteration testing method and rapid testing method. The system's efficiency with the four algorithms is compared and analyzed along with tracking speed and efficiency under all irradiance circumstances. The simulated results show that the ARO algorithm, which locates MPP at 86.8 W with 99.86% efficiency, is better among all the other algorithms under no shading conditions. The MVP algorithm tracks slightly better results in slightly shaded and rapidly shaded conditions in terms of efficiency. So, this study suggests that the ARO algorithm for standard testing conditions and based on the results obtained from Case 2 and Case 3, the MVP algorithm is a better option for change in operating conditions. Finally, this study concludes that the MVP algorithm is better in all aspects and can be an alternative tool for MPPT applications.




REFERENCES

- [1] E. Romero-Cadaval, G. Spagnuolo, L. G. Franquelo, C. A. Ramos-Paja, T. Suntio, and W. M. Xiao, "Grid-connected photovoltaic generation plants: Components and operation," *IEEE Industrial Electronics Magazine*, vol. 7, no. 3, pp. 6–20, 2013, doi: 10.1109/MIE.2013.2264540.
- [2] M. Premkumar, C. Kumar, and R. Sowmya, "Mathematical modelling of solar photovoltaic cell/panel/array based on the physical parameters from the manufacturer's datasheet," *International Journal of Renewable Energy Development*, vol. 9, no. 1, pp. 7–22, 2020, doi: 10.14710/ijred.9.1.7-22.
- [3] B. Subudhi and R. Pradhan, "A comparative study on maximum power point tracking techniques for photovoltaic power systems," *IEEE Transactions on Sustainable Energy*, vol. 4, no. 1, pp. 89–98, Jan. 2013, doi: 10.1109/TSTE.2012.2202294.
- [4] M. Premkumar and R. Sowmya, "An effective maximum power point tracker for partially shaded solar photovoltaic systems," *Energy Reports*, vol. 5, pp. 1445–1462, 2019, doi: 10.1016/j.egy.2019.10.006.
- [5] C. Gonzalez-Castano, C. Restrepo, S. Kouro, and J. Rodriguez, "MPPT Algorithm Based on Artificial Bee Colony for PV System," *IEEE Access*, vol. 9, pp. 43121–43133, 2021, doi: 10.1109/ACCESS.2021.3066281.
- [6] M. A. Elgendy, B. Zahawi, and D. J. Atkinson, "Assessment of the incremental conductance maximum power point tracking algorithm," *IEEE Transactions on Sustainable Energy*, vol. 4, no. 1, pp. 108–117, 2013, doi: 10.1109/TSTE.2012.2202698.
- [7] M. A. Elgendy, B. Zahawi, and D. J. Atkinson, "Assessment of perturb and observe MPPT algorithm implementation techniques for PV pumping applications," *IEEE Transactions on Sustainable Energy*, vol. 3, no. 1, pp. 21–33, 2012, doi: 10.1109/TSTE.2011.2168245.
- [8] H. Patel and V. Agarwal, "Maximum power point tracking scheme for PV systems operating under partially shaded conditions," *IEEE Transactions on Industrial Electronics*, vol. 55, no. 4, pp. 1689–1698, 2008, doi: 10.1109/TIE.2008.917118.
- [9] P. Manoharan *et al.*, "Improved Perturb and Observation Maximum Power Point Tracking Technique for Solar Photovoltaic Power Generation Systems," *IEEE Systems Journal*, vol. 15, no. 2, pp. 3024–3035, Jun. 2021, doi: 10.1109/JSYST.2020.3003255.
- [10] A. Al Nabulsi and R. Dhaouadi, "Efficiency optimization of a dsp-based standalone PV system using fuzzy logic and dual-MPPT control," *IEEE Transactions on Industrial Informatics*, vol. 8, no. 3, pp. 573–584, 2012, doi: 10.1109/TII.2012.2192282.
- [11] Syafaruddin, E. Karatepe, and T. Hiyama, "Artificial neural network-polar coordinated fuzzy controller based maximum power point tracking control under partially shaded conditions," *IET Renewable Power Generation*, vol. 3, no. 2, pp. 239–253, 2009, doi: 10.1049/iet-rpg:20080065.
- [12] L. M. Elobaid, A. K. Abdelsalam, and E. E. Zakzouk, "Artificial neural network-based photovoltaic maximum power point tracking techniques: A survey," *IET Renewable Power Generation*, vol. 9, no. 8, pp. 1043–1063, 2015, doi: 10.1049/iet-rpg.2014.0359.
- [13] R. B. Roy, J. Cros, A. Nandi, and T. Ahmed, "Maximum Power Tracking by Neural Network," *ICRITO 2020 - IEEE 8th International Conference on Reliability, Infocom Technologies and Optimization (Trends and Future Directions)*, 2020, pp. 89–93, doi: 10.1109/ICRITO48877.2020.9197882.
- [14] N. Kumar, I. Hussain, B. Singh, and B. K. Panigrahi, "Rapid MPPT for Uniformly and Partial Shaded PV System by Using JayaDE Algorithm in Highly Fluctuating Atmospheric Conditions," *IEEE Transactions on Industrial Informatics*, vol. 13, no. 5, pp. 2406–2416, 2017, doi: 10.1109/TII.2017.2700327.
- [15] M. Seyedmahmoudian *et al.*, "Simulation and Hardware Implementation of New Maximum Power Point Tracking Technique for Partially Shaded PV System Using Hybrid DEPSO Method," *IEEE Transactions on Sustainable Energy*, vol. 6, no. 3, pp. 850–862, 2015, doi: 10.1109/TSTE.2015.2413359.
- [16] A. M. Eltamaly, M. S. Al-Saud, A. G. Abokhalil, and H. M. H. Farh, "Simulation and experimental validation of fast adaptive particle swarm optimization strategy for photovoltaic global peak tracker under dynamic partial shading," *Renewable and Sustainable Energy Reviews*, vol. 124, p. 109719, May 2020, doi: 10.1016/j.rser.2020.109719.
- [17] M. Alshareef, Z. Lin, M. Ma, and W. Cao, "Accelerated particle swarm optimization for photovoltaic maximum power point tracking under partial shading conditions," *Energies*, vol. 12, no. 4, 2019, doi: 10.3390/en12040623.
- [18] M. Joisher, D. Singh, S. Taheri, D. R. Espinoza-Trejo, E. Pouresmaeil, and H. Taheri, "A Hybrid Evolutionary-Based MPPT for Photovoltaic Systems under Partial Shading Conditions," *IEEE Access*, vol. 8, pp. 38481–38492, 2020, doi: 10.1109/ACCESS.2020.2975742.
- [19] M. Bounabi, K. Kaced, M. S. Ait-Cheikh, C. Larbes, Z. E. Dahmane, and N. Ramzan, "Modelling and performance analysis of different multilevel inverter topologies using PSO-MPPT technique for grid connected photovoltaic systems," *Journal of Renewable and Sustainable Energy*, vol. 10, no. 4, 2018, doi: 10.1063/1.5043067.
- [20] D. F. Teshome, C. H. Lee, Y. W. Lin, and K. L. Lian, "A modified firefly algorithm for photovoltaic maximum power point tracking control under partial shading," *IEEE Journal of Emerging and Selected Topics in Power Electronics*, vol. 5, no. 2, pp. 661–671, 2017, doi: 10.1109/JESTPE.2016.2581858.
- [21] S. Krishnan G, S. Kinattingal, S. P. Simon, and P. S. R. Nayak, "MPPT in PV systems using ant colony optimisation with dwindling population," *IET Renewable Power Generation*, vol. 14, no. 7, pp. 1105–1112, May 2020, doi: 10.1049/iet-rpg.2019.0875.
- [22] J. Prasanth Ram and N. Rajasekar, "A Novel Flower Pollination Based Global Maximum Power Point Method for Solar Maximum Power Point Tracking," *IEEE Transactions on Power Electronics*, vol. 32, no. 11, pp. 8486–8499, Nov. 2017, doi: 10.1109/TPEL.2016.2645449.
- [23] C. Huang, Z. Zhang, L. Wang, Z. Song, and H. Long, "A novel global maximum power point tracking method for PV system using Jaya algorithm," *2017 IEEE Conference on Energy Internet and Energy System Integration, EI2 2017 - Proceedings*, 2017, pp. 1–5, doi: 10.1109/EI2.2017.8245345.
- [24] K. S. Tey, S. Mekhilef, M. Seyedmahmoudian, B. Horan, A. T. Oo, and A. Stojcevski, "Improved Differential Evolution-Based MPPT Algorithm Using SEPIC for PV Systems Under Partial Shading Conditions and Load Variation," *IEEE Transactions on Industrial Informatics*, vol. 14, no. 10, pp. 4322–4333, 2018, doi: 10.1109/TII.2018.2793210.
- [25] S. Mohanty, B. Subudhi, and P. K. Ray, "A Grey Wolf-Assisted Perturb & Observe MPPT Algorithm for a PV System," *IEEE Transactions on Energy Conversion*, vol. 32, no. 1, pp. 340–347, 2017, doi: 10.1109/TEC.2016.2633722.
- [26] M. Seyedmahmoudian, T. K. Soon, B. Horan, A. Ghandhari, S. Mekhilef, and A. Stojcevski, "New ARMO-based MPPT Technique to Minimize Tracking Time and Fluctuation at Output of PV Systems under Rapidly Changing Shading Conditions," *IEEE Transactions on Industrial Informatics*, pp. 1–1, 2019, doi: 10.1109/tii.2019.2895066.




- [27] D. Yousri, T. S. Babu, D. Allam, V. K. Ramachandaramurthy, and M. B. Etiba, "A novel chaotic flower pollination algorithm for global maximum power point tracking for photovoltaic system under partial shading conditions," *IEEE Access*, vol. 7, pp. 121432–121445, 2019, doi: 10.1109/ACCESS.2019.2937600.
- [28] S. Veerapen *et al.*, "A novel global maximum power point tracking algorithm for photovoltaic system with variable perturbation frequency and zero oscillation," *Solar Energy*, vol. 181, pp. 345–356, 2019, doi: 10.1016/j.solener.2019.01.082.
- [29] H. Chaieb and A. Sakly, "A novel MPPT method for photovoltaic application under partial shaded conditions," *Solar Energy*, vol. 159, pp. 291–299, 2018, doi: 10.1016/j.solener.2017.11.001.
- [30] K. Wang, J. Ma, K. L. Man, K. Huang, and X. Huang, "Comparative study of modern heuristic algorithms for global maximum power point tracking in photovoltaic systems under partial shading conditions," *Frontiers in Energy Research*, vol. 10, 2022, doi: 10.3389/fenrg.2022.946864.
- [31] M. Kermadi *et al.*, "Recent developments of mppt techniques for pv systems under partial shading conditions: A critical review and performance evaluation," *IET Renewable Power Generation*, vol. 14, no. 17, pp. 3401–3417, 2020, doi: 10.1049/iet-rpg.2020.0454.
- [32] A. M. Eltamaly, "An improved cuckoo search algorithm for maximum power point tracking of photovoltaic systems under partial shading conditions," *Energies*, vol. 14, no. 4, 2021, doi: 10.3390/en14040953.
- [33] M. N. Bhukya and V. R. Kota, "A quick and effective MPPT scheme for solar power generation during dynamic weather and partial shaded conditions," *Engineering Science and Technology, an International Journal*, vol. 22, no. 3, pp. 869–884, 2019, doi: 10.1016/j.jestech.2019.01.015.
- [34] M. Premkumar and R. Sumithira, "Humpback whale assisted hybrid maximum power point tracking algorithm for partially shaded solar photovoltaic systems," *Journal of Power Electronics*, vol. 18, no. 6, pp. 1805–1818, 2018, doi: 10.6113/JPE.2018.18.6.1805.
- [35] M. Premkumar, C. Kumar, A. Anbarasan, and R. Sowmya, "A new maximum power point tracking technique based on whale optimisation algorithm for solar photovoltaic systems," *International Journal of Ambient Energy*, vol. 43, no. 1, pp. 5627–5637, 2022, doi: 10.1080/01430750.2021.1969270.
- [36] M. Mao *et al.*, "A hybrid intelligent GMPPT algorithm for partial shading PV system," *Control Engineering Practice*, vol. 83, pp. 108–115, 2019, doi: 10.1016/j.conengprac.2018.10.013.
- [37] S. Sarwar *et al.*, "A Novel Hybrid MPPT Technique to Maximize Power Harvesting from PV System under Partial and Complex Partial Shading," *Applied Sciences (Switzerland)*, vol. 12, no. 2, 2022, doi: 10.3390/app12020587.
- [38] D. Pilakkat and S. Kanthalakshmi, "An improved P&O algorithm integrated with artificial bee colony for photovoltaic systems under partial shading conditions," *Solar Energy*, vol. 178, pp. 37–47, 2019, doi: 10.1016/j.solener.2018.12.008.
- [39] S. Padmanaban, N. Priyadarshi, M. S. Bhaskar, J. B. Holm-Nielsen, E. Hossain, and F. Azam, "A Hybrid Photovoltaic-Fuel Cell for Grid Integration with Jaya-Based Maximum Power Point Tracking: Experimental Performance Evaluation," *IEEE Access*, vol. 7, pp. 82978–82990, 2019, doi: 10.1109/ACCESS.2019.2924264.
- [40] M. A. Hassan, N. Bailek, K. Bouchouicha, and S. C. Nwokolo, "Ultra-short-term exogenous forecasting of photovoltaic power production using genetically optimized non-linear auto-regressive recurrent neural networks," *Renewable Energy*, vol. 171, pp. 191–209, 2021, doi: 10.1016/j.renene.2021.02.103.
- [41] M. A. Hassan *et al.*, "Evaluation of energy extraction of PV systems affected by environmental factors under real outdoor conditions," *Theoretical and Applied Climatology*, vol. 150, no. 1–2, pp. 715–729, 2022, doi: 10.1007/s00704-022-04166-6.
- [42] S. C. Nwokolo, A. U. Obiwulu, and J. C. Ogbulezie, "Machine learning and analytical model hybridization to assess the impact of climate change on solar PV energy production," *Physics and Chemistry of the Earth*, vol. 130, 2023, doi: 10.1016/j.pce.2023.103389.
- [43] H. R. E. H. Boucekara, "Most Valuable Player Algorithm: a novel optimization algorithm inspired from sport," *Operational Research*, vol. 20, no. 1, pp. 139–195, Mar. 2020, doi: 10.1007/s12351-017-0320-y.
- [44] I. Pervez, I. Shams, S. Mekhilef, A. Sarwar, M. Tariq, and B. Alamri, "Most Valuable Player Algorithm based Maximum Power Point Tracking for a Partially Shaded PV Generation System," *IEEE Transactions on Sustainable Energy*, vol. 12, no. 4, pp. 1876–1890, 2021, doi: 10.1109/TSTE.2021.3069262.
- [45] L. Wang, Q. Cao, Z. Zhang, S. Mirjalili, and W. Zhao, "Artificial rabbits optimization: A new bio-inspired meta-heuristic algorithm for solving engineering optimization problems," *Engineering Applications of Artificial Intelligence*, vol. 114, 2022, doi: 10.1016/j.engappai.2022.105082.
- [46] M. Premkumar, P. Jangir, and R. Sowmya, "Parameter extraction of three-diode solar photovoltaic model using a new metaheuristic resistance-capacitance optimization algorithm and improved Newton–Raphson method," *Journal of Computational Electronics*, vol. 22, no. 1, pp. 439–470, 2023, doi: 10.1007/s10825-022-01987-6.

BIOGRAPHIES OF AUTHORS






Suraj Ravi    was born in Shimoga, India. He received a B.E. degree in electrical and electronics from SDM Institute of Technology, Ujire, affiliated with VTU University Belgaum, India, during 2015–2019, and is currently pursuing M.Tech. degree in Power Electronics from the Dayananda Sagar College of Engineering, Bengaluru, Karnataka, India. His field of interest is MPPT techniques, optimization algorithms, and DC-DC power converters. He can be contacted at email: surajravi771997@gmail.com.



Manoharan Premkumar    was born in Coimbatore, India. He received a B.E. degree in electrical and electronics engineering from the Sri Ramakrishna Institute of Technology, Coimbatore, in 2004, an M.E. degree in applied electronics from the Anna University of Technology, Coimbatore, in 2010, and the Ph.D. degree from Anna University, Chennai, India, in 2019. He is currently working as an Associate Professor with the Dayananda Sagar College of Engineering, Bengaluru, India. He has over 14 years of teaching experience. He has published over 110 technical articles in various national/international peer-reviewed journals, such as IEEE, Elsevier, and Springer, with over 1800 citations and an H-index of 22. He has published/granted seven patents by IPR, India, and IPR, Australia. His current research interests include optimization algorithms, including single-, multi-, and many-objectives for different real-world engineering design problems, power converters/inverters, PV parameter extraction, PV MPPT, PV array faults, smart grid and microgrids, BMS for electric vehicles, and non-isolated/isolated DC-DC converters for renewable energy systems and EVs. According to the report published by Stanford University in 2021, he is one of the 2% influential scholars, which depicts the 100000 top scientists in the world. He is a member of various professional bodies, such as IEEE, ISTE, and IAENG. He is also an editor/reviewer for leading journals of different publishers, such as IEEE, IET, Wiley, Taylor & Francis, Springer, and MDPI. He can be contacted at email: mprem.me@gmail.com.



Laith Abualigah    received a degree in computer information systems and a master's degree in computer science from Al-Albayt University, Jordan, in 2011 and 2014, respectively, and the Ph.D. degree from the School of Computer Science, Universiti Sains Malaysia (USM), Malaysia, in 2018. He is currently an Associate Professor with the Computer Science Department, Prince Hussein Bin Abdullah Faculty for Information Technology, Al al-Bayt University, Mafrq 25113, Jordan. He is also affiliated with the Hourani Center for Applied Scientific Research, Al-Ahliyya Amman University, Amman 19328, Jordan, MEU Research Unit, Middle East University, Amman, Jordan, and School of Computer Sciences, Universiti Sains Malaysia, Pulau Pinang 11800, Malaysia. According to the report published by Stanford University in 2020, he is one of the 2% influential scholars, which depicts the 100000 top scientists in the world. He has published more than 200 journal articles and books, which collectively have been cited more than 12264 times (H-index = 53). His main research interests include arithmetic optimization algorithm (AOA), bio-inspired computing, nature-inspired computing, swarm intelligence, artificial intelligence, meta-heuristic modelling and optimization algorithms, evolutionary computations, information retrieval, text clustering, feature selection, combinatorial problems, optimization, advanced machine learning, big data, and natural language processing. He also serves as an Associate Editor for the Cluster Computing journal (Springer) and the Soft Computing journal (Springer). He can be contacted at email: aligah.2020@gmail.com.